Dielectric and complex impedance studies of $BaTi_{0.85}W_{0.15}O_{3+\delta}$ ferroelectric ceramics

SHEELA DEVI and A K JHA[*]

Department of Applied Physics, Delhi College of Engineering, Faculty of Technology, University of Delhi, Delhi 110 042, India

Abstract. In the present work, tungsten substituted barium titanate have been synthesized and studied. The structural analysis indicates that the specimen is a single phase material with tetragonal crystal structure. The observed polarization–electric field hysteresis loop confirms the ferroelectric nature of the prepared compound. Variation of dielectric constant with temperature at different frequencies shows that the compound has a dielectric anomaly at 75 °C and exhibits diffuse type phase transition. Variation of dielectric loss with temperature at different frequencies shows a decrease in loss with increasing frequency. The Nyquist plots (Cole–Cole plots) have been measured at temperatures 325 °C, 345 °C and 365 °C. The plot at 365 °C shows a grain boundary effect. Relaxation time has been found to decrease with the rise in temperature and obey the Arrhenius relationship. The variations of d.c. conductivity as a function of temperature have also been studied.

Keywords. Ferroelectrics; grain boundaries; dielectric response; X-ray diffraction.

1. Introduction

Since the discovery of $BaTiO_3$, these materials have been extensively studied owing to their interesting dielectric, ferroelectric, piezoelectric and pyroelectric properties (Goodman and Buchanan 1986; Hench and West 1990; Reynolds 2001). Barium titanate is an important electroceramic due to its applications in multilayer ceramic capacitor (MLCC), positive temperature coefficient of resistance (PTCR) thermisters, piezoelectric sensors, transducers and electro-optic devices (Jaffe *et al* 1971; Jones *et al* 1992; Hu and Krupanidhi 1993; Haertling 1999). Being Pb free, it is an environment friendly material making it a good substitute for Pb containing compounds for various applications. It is a typical ferroelectric material with Curie temperature in the range of 120–130 °C (Megaw 1945; Devi *et al* 2009). $BaTiO_3$ has a perovskite (ABO_3) tetragonal structure at room temperature and when heated beyond T_c, from ferroelectric to paraelectric phase, its structure changes from tetragonal to cubic (Merz 1949; Zaffe *et al* 1971).

Complex impedance spectroscopy (CIS) technique is a useful experimental technique for correlating the dielectric and electrical characteristics in ceramics (Ganguly *et al* 2008). It is reported that partial substitution of W is effective in enhancing the dielectric and ferroelectric properties of $SrBi_2Ta_2O_9$ (Coondoo *et al* 2006, 2007a, b). The present work was undertaken with an objective of investigating the effect of partial substitution of Ti by W and its effect on the electrical characteristics of $BaTiO_3$. Although $BaTiO_3$ is a widely studied material, however, hardly any report is available in the literature on the complex impedance spectroscopy analysis of tungsten substituted barium titanate. The present report summarizes the results of an extensive study on the electrical characteristics including complex impedance spectroscopy of $BaTi_{0.85}W_{0.15}O_{3+\delta}$ ferroelectric ceramic.

2. Experimental

Sample of composition, $BaTi_{0.85}W_{0.15}O_{3+\delta}$, was prepared using solid state reaction technique taking $BaCO_3$, TiO_2 and WO_3 (all from Aldrich with 99·9% purity) in stoichiometric proportions. The powders were thoroughly mixed, grounded and passed through sieves of appropriate sizes. The mixture was calcined at 1150 °C for 2 h in air. The calcined specimen was mixed with appropriate quantity of polyvinyl alcohol and molded into disc shape pellets by applying a pressure of 300 MPa. The pellets were sintered at 1250 °C for 2 h.

X-ray diffractogram of the sintered sample was recorded on a Philips X-ray diffractometer using CuK_α radiation ($\lambda = 1·5405$ Å) in the range $10° \leq 2\theta \leq 70°$ at a scanning rate of 0·02°/s. The sintered pellets were polished to a thickness of 1 mm, coated with silver paste on both sides for use as electrodes and finally cured at 300 °C for 15 min. Scanning electron micrograph (SEM) of the sample was recorded using Cambridge Stereo Scan 360 microscope. The dielectric parameters were mea-

*Author for correspondence (dr_jha_ak@yahoo.co.in)

sured from 100 Hz–1 MHz on an Agilent 4284A LCR meter at an oscillation amplitude of 1 V. The impedance measurements were carried out in the temperature range 325–365 °C at an interval of 20 °C using Agilent 4284A precision LCR meter in the frequency range 20 Hz–1 MHz. Polarization–electric field (P–E) hysteresis loop was recorded at room temperature using an automatic P–E loop tracer based on Sawyer–Tower circuit.

3. Results and discussion

3.1 *Structural and ferroelectric analysis*

Figure 1 shows the X-ray diffraction pattern of the studied sample. It is observed that a single phase perovskite structure is formed. The lattice parameters were calculated using the observed interplanar spacing d values from the diffractogram and refined using the least square refinement method by a computer program package Powder-X (Dong 1999). The obtained lattice parameters are: $a=b=3\cdot994$ Å and $c=4\cdot019$ Å with $c/a=1\cdot006$. The unit cell volume is found to be $64\cdot11$ (Å)^3. A reduction in the lattice parameters of tungsten substituted barium titanate is observed compared to tungsten free barium titanate reported elsewhere (Devi *et al* 2009), indicating that the added tungsten atoms occupy *B*-sites, as expected on the basis of ionic radius and coordination number (Shannon and Prewitt 1969). The peaks have been indexed using the observed d-values and the calculated lattice parameters. From these, it is found that the studied specimen has a tetragonal perovskite structure.
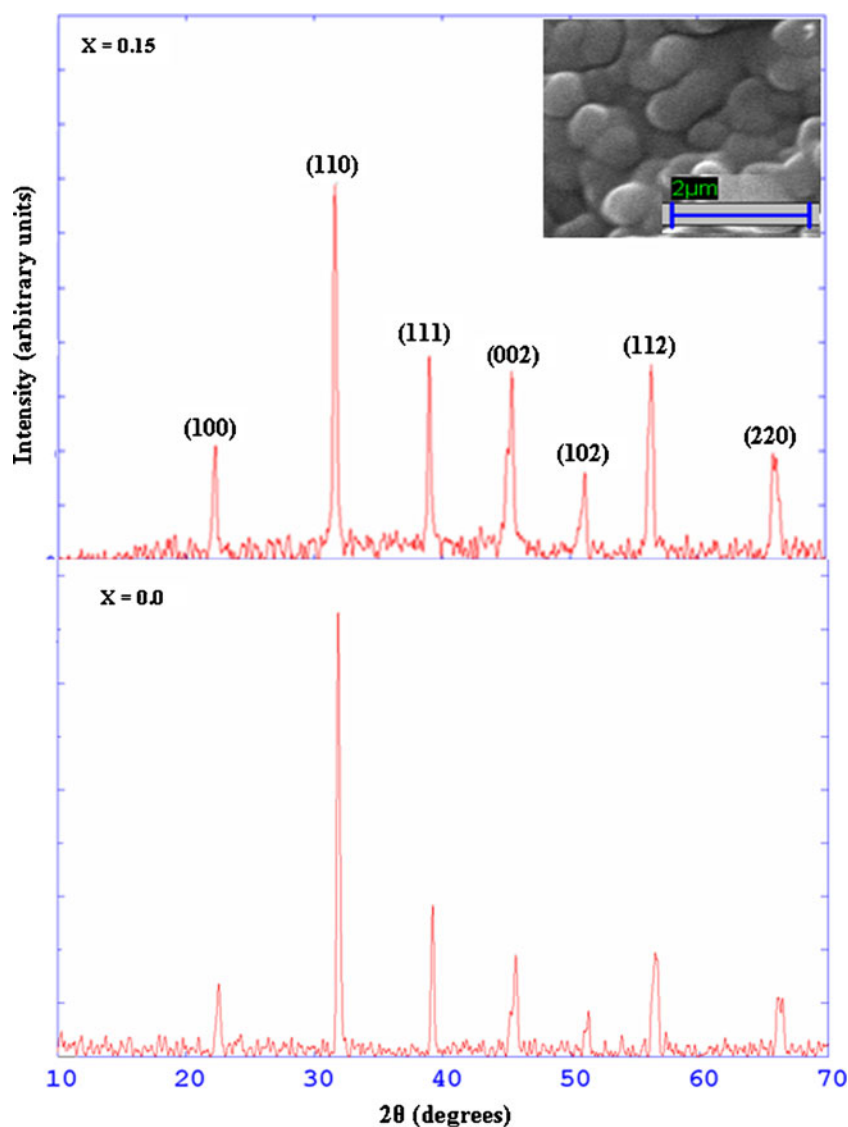

Figure 1. X-ray diffraction patterns of BaTi$_{1-x}$W$_x$O$_{3+\delta}$ compound and SEM micrograph of W containing specimen (inset).

The SEM micrograph of the specimen is also shown in the inset of figure 1. Well developed randomly oriented grains are observed in the micrograph.

The ferroelectric nature of the prepared sample was confirmed by P–E hysteresis loop (figure 2). The observed values of remanent polarization (P_r) and coercive field (E_c) are 1·8 μC/cm^2 and 2·2 kV/cm, respectively while the saturation polarization (P_s) is observed to be around 8 μC/cm^2. Tungsten substitution, i.e. donor doping, induces 'soft' nature in the material resulting in higher saturation polarization, P_s and lower remnance polarization as the movements of the domains become easier (Stojanovic *et al* 2004).

3.2 *Dielectric characterization*

Figure 3 shows the variation of dielectric constant of the studied specimen with temperature at different frequencies. The ferroelectric to paraelectric transitions are observed at the same Curie temperature, where dielectric constant is maximum, at all frequencies indicating non-relaxor behaviour. It is observed that the T_c decreases to 75 °C as compared to 120 °C in the pure sample on partially replacing titanium by tungsten. The possible reason for the decrease in Curie temperature is as follows. On tungsten substitution there is reduction in Curie temperature because on substitution of tungsten for titanium at *B*-site, the bonding energy between *B*-site and oxygen octahedral of ABO$_3$ pervoskite structure reduces. This decrease in bonding energy leads to weaker distortion of the octahedron. Also, due to smaller ionic radius of W as compared to Ti, there is a decrease in *c*/*a* ratio. These factors are responsible for the observed reduction in Curie temperature (Cao *et al* 2007).

The dielectric constant of tungsten containing sample is found to be higher as compared to the pure sample (Devi *et al* 2009) and the dielectric constant decreases with increase
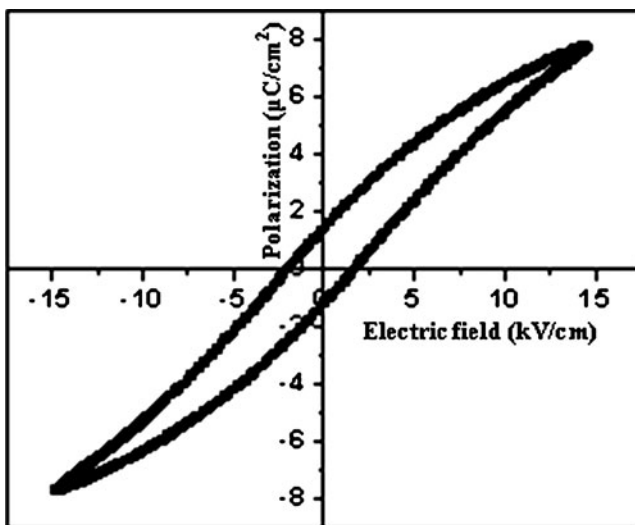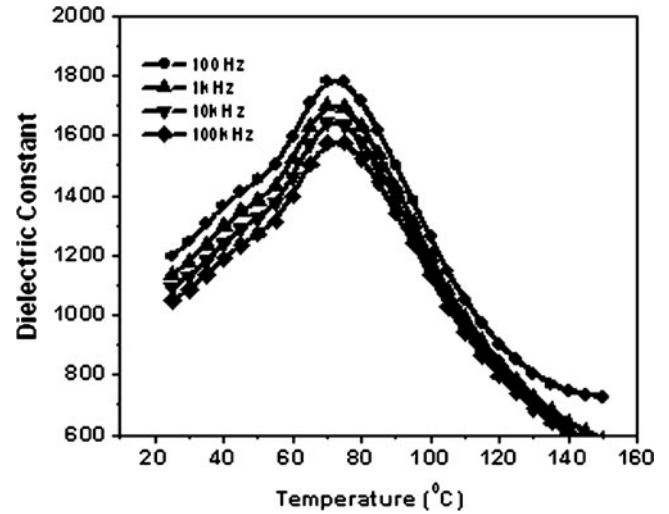

Figure 3. Variation of dielectric constant with temperature at different frequencies.
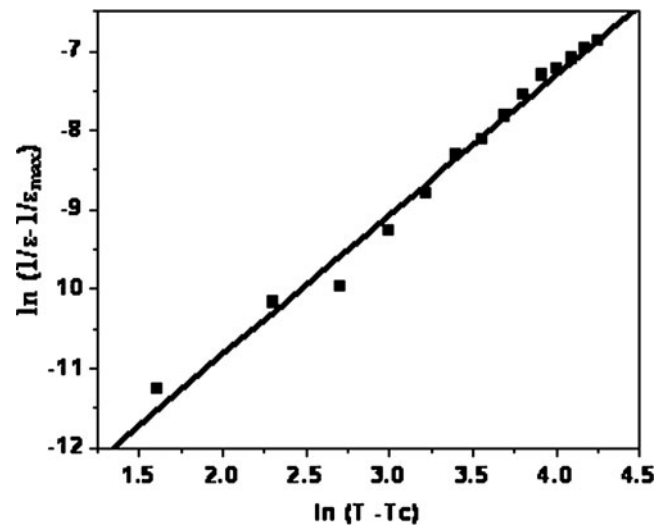

Figure 4. Variation of ln ($1/\varepsilon - 1/\varepsilon_{max}$) with ln ($T - T_c$) at 100 kHz.

in frequencies. The observed reduction of dielectric constant at higher frequencies is possibly due to the easy depolarization of dipoles that exist at the weak bonded interface and boundary regions (Viswanath and Ramasamy 1997). The increase of dielectric constant on tungsten substitution can be understood as follows. It is known that when a higher valent ion is substituted for lower valent ion, cation vacancies are generated to maintain the charge neutrality of the structure (Zhang *et al* 2004; Coondoo *et al* 2007a, b). The defect formation is represented as

$$\text{Null} = W_{\text{Ti}}^{\cdot\cdot} + V_{\text{Ba}}^{''}, \tag{1}$$

where, V_{Ba} denotes the barium vacant site. These cationic vacancies generated by donor doping facilitates the switching of the domain walls, which ultimately lead to the increase of dielectric constant (Wu *et al* 2002).
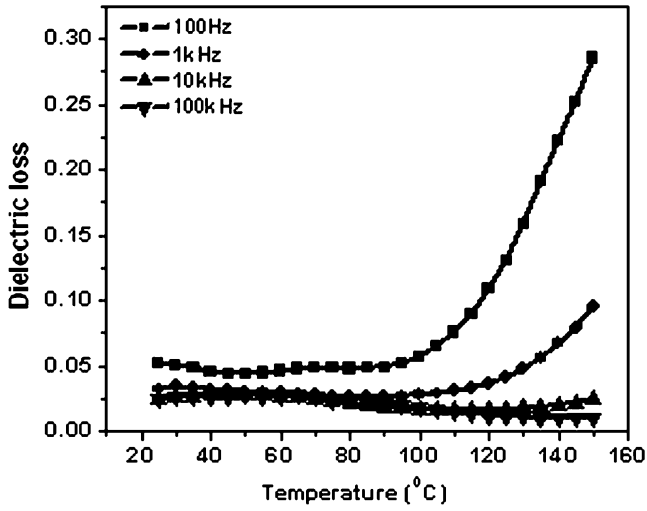

Figure 2. Polarization hysteresis curve of BaTi$_{0.85}$W$_{0.15}$O$_{3+\delta}$.

Figure 5. Variation of dielectric loss with temperature at different frequencies.
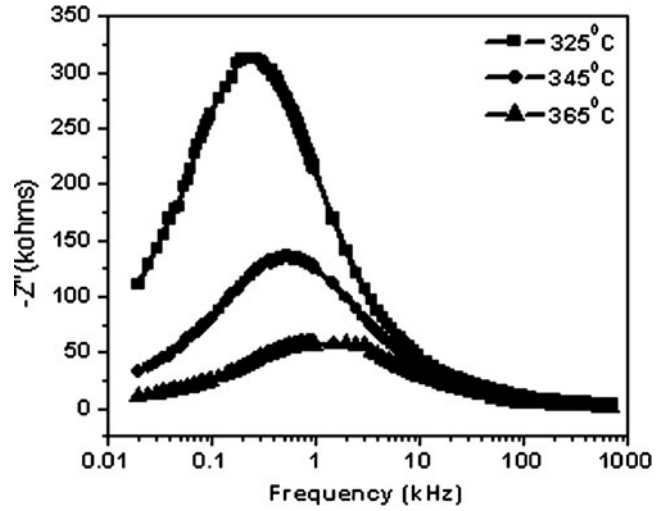

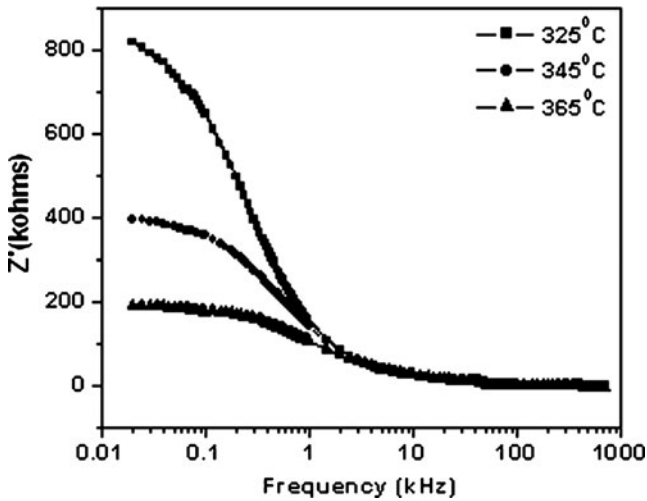**Figure 7.** Variation of imaginary part of impedance (Z'') with frequency at different temperatures.

Figure 6. Variation of real part of impedance (Z') with frequency at different temperatures.
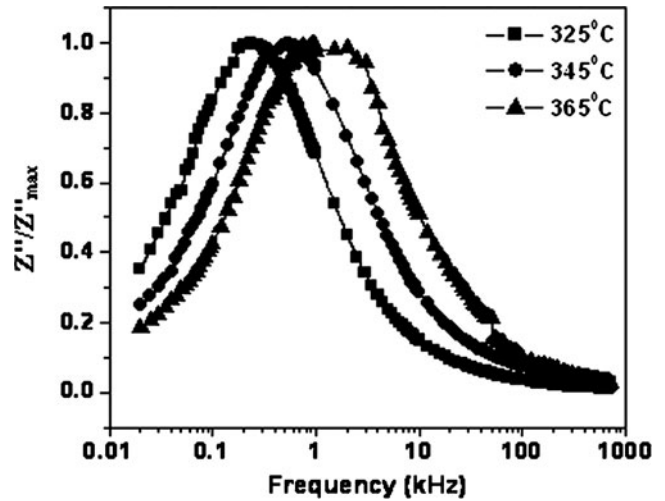

Figure 8. Normalized imaginary part of impedance (Z''/ Z''_{max}) as a function of frequency at several temperatures.

Figure 4 shows the variation of ln ($1/ \varepsilon - 1/ \varepsilon_{max}$) with ln ($T-T_c$) at a frequency of 100 kHz. It is observed (figure 3) that the dielectric peak is broadened indicating a diffuse kind of phase transition. Diffusivity in the sample is calculated by using the expression (Pilgrim *et al* 1990)

$$\ln(1/\varepsilon - 1/\varepsilon_{max}) = \gamma \ln(T - T_c) + \text{constant}, \qquad (2)$$

where ε_{max} is the maximum dielectric constant at 100 kHz and γ the diffusivity or disorderness of ferroelectric to paraelectric phase transition, and its value lies between 1 and 2 (Xiong *et al* 2004). The value of γ is calculated from the slope of the curve and is found to be 1·76. When $\gamma=1$, the material follows an ideal Curie–Weiss law as in the case of normal ferroelectric, whereas when $\gamma=2$ the material

corresponds to a complete diffuse phase transition (DPT) (Uchino and Nomura 1982). The observed value of $\gamma=1·76$ indicates a largely diffused kind of phase transition.

Figure 5 shows the variation of dielectric loss with temperature at different frequencies. It shows negligible change up to 100 °C, largely independent of temperature, thereafter, it increases with temperature. The loss is observed to be higher at lower frequency. This can be understood from the fact that at the lower frequencies the dipoles are able to follow the variations of the applied alternating electric field resulting in the higher dielectric loss. Further, the dielectric loss is observed to increase on tungsten substitution, which is possibly due to the domain boundary vibrations or excitations that are readily stimulated under weak a.c. drive conditions (Zong *et al* 2004).
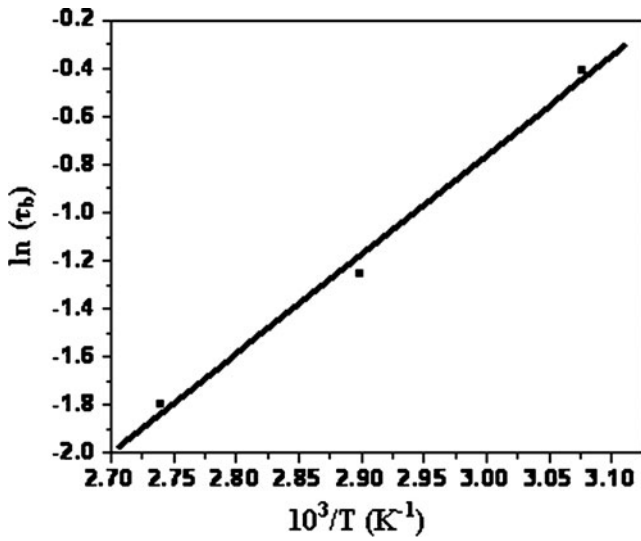
Figure 9. Variation of ln (τ_b) with inverse of absolute temperature ($10^3/T$).

4. Impedance studies

The complex impedance study is an informative and powerful technique in materials research which gives vital information regarding the distribution parameters of different micro regions in the polycrystalline materials, such as grain, grain boundary and electrode interface (Sinclair and West 1989, 1994). Different mechanisms involved in the relaxation as well as in a.c. conduction process can be resolved by plotting the impedance at different frequencies in a complex plane and is found very effective in separating the contributions of various factors such as bulk effect, grain boundary effect and interfaces. The electrical properties are determined, in general, by a series of combinations of such impedances. Each of these components is represented by a parallel RC element (Venkateswarlu *et al* 2005). A polycrystalline material usually shows both grain and grain boundary effects with different time constants leading to two successive semi-
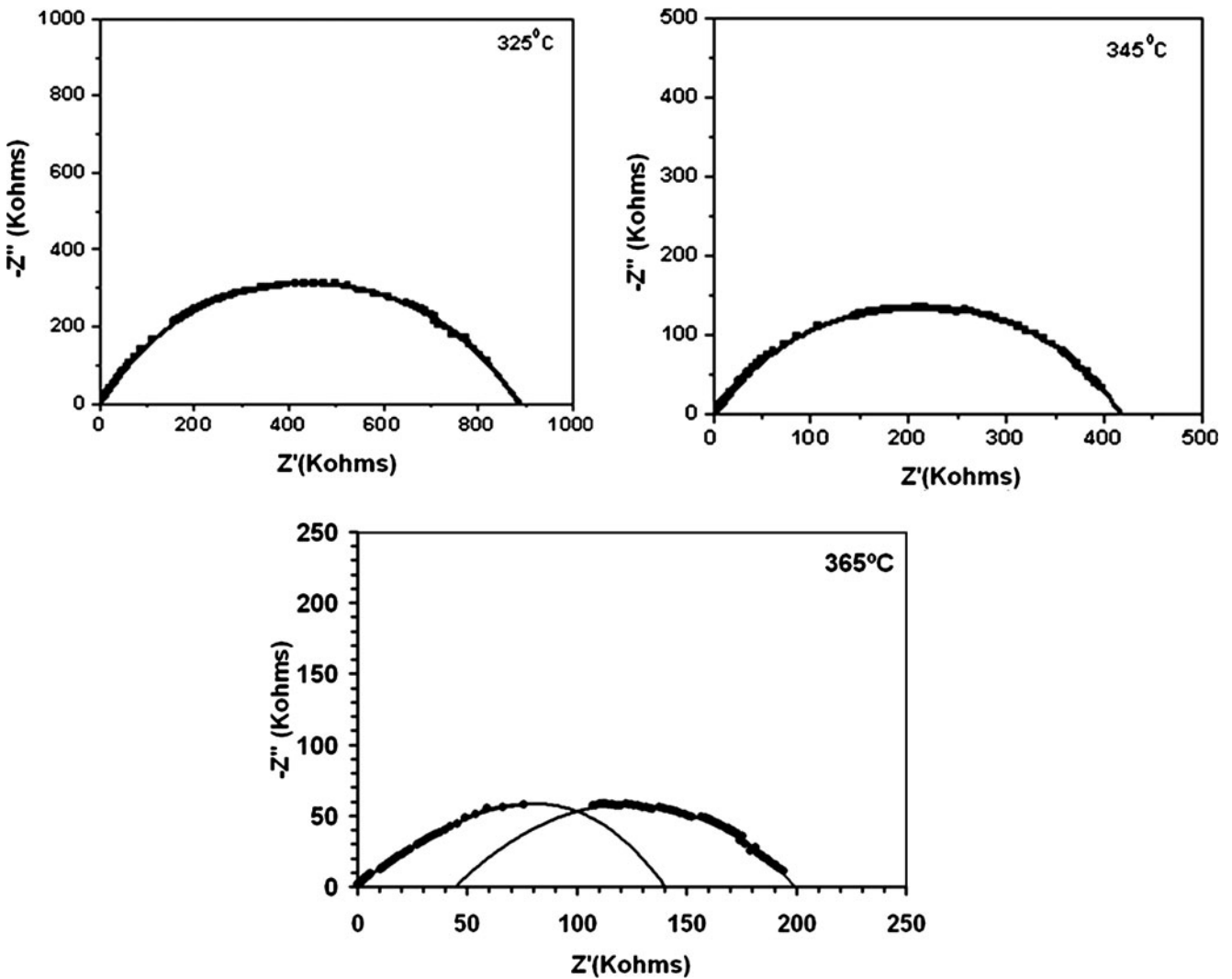

Figure 10. Complex impedance spectrum (Cole–Cole plots) of $BaTi_{0.85}W_{0.15}O_{3+\delta}$ at different temperatures.

Table 1. Bulk resistance (R_b), bulk capacitance (C_b), grain boundary resistance (R_{gb}) and grain boundary capacitance (C_{gb}) of the studied samples.

Temperature (°C)	R_b (KΩ)	C_b (nF)	R_{gb} (KΩ)	C_{gb} (nF)
325	885	0·74	-	-
345	420	0·68	-	-
365	140	0·12	200	0·83

circles (Behera *et al* 2007). The electrical properties of a material are often expressed in terms of some complex parameters like complex impedance (Z^*), complex admittance (Y^*), complex permittivity (ε^*) and dielectric loss (tan δ). These frequency dependent parameters are related to each other by the following relations:

$$Z^*(\omega) = Z' - j\,Z'' = R_s - \frac{j}{\omega C_s} = \frac{1}{j\omega C_0 \varepsilon^*}, \qquad (3)$$

$$Y^*(\omega) = Y' + j\,Y'' = \frac{1}{R_p} + j\omega C_p = j\omega C_0 \varepsilon^* = \frac{1}{Z^*}, \quad (4)$$

$$\varepsilon^*(\omega) = \varepsilon' - j\varepsilon'', \qquad (5)$$

$$\tan\delta = \frac{Z'}{Z''} = \frac{Y'}{Y''} = \frac{\varepsilon''}{\varepsilon'}, \qquad (6)$$

where R_s, C_s are the series resistance and capacitance, R_p, C_p the parallel resistance and capacitance, C_0 the geometrical capacitance, (Z', Y', ε') and (Z'', Y'', ε'') are the real and imaginary components of impedance, admittance and permittivity, respectively ($j = \sqrt{-1}$).

Figure 6 shows the variation of real part of impedance (Z') with frequency at different temperatures. The impedance value is higher at lower temperature in the low frequency range and decreases gradually with increasing frequency. It is observed that the value of Z' decreases with the increase of both frequency and temperature, which indicates that the conduction is increasing with the increase of temperature and frequency. The values of Z' coincide in the higher frequency region at all temperatures. It is possibly related to the release of space charge with the rise of temperature and is responsible for the enhancement of conduction in the material with temperature at higher frequencies. This is in conformity with the observed higher impedance values at lower frequencies (Sen *et al* 2007).

Figure 7 shows the variation of Z'' with frequency at different temperatures. The plots show that Z'' values attain a peak (Z''_{max}) at all the measured temperatures, which shifts to higher frequency with increasing temperature and all the curves merge at higher frequencies. The shifting of peaks

towards higher frequency indicates that the relaxation time is decreasing with the increase of temperature (Behera *et al* 2008). The peak broadening with increasing temperature suggests the presence of temperature dependent electrical relaxation phenomenon in the material (Behera *et al* 2007). The relaxation process is due to the presence of space charges whose mobility increases at higher temperature (Sen *et al* 2007).

Figure 8 shows the variation of (Z''/Z''_{max}) with frequency at temperatures of measurement. The curves show a peak with a slightly asymmetric broadening at each temperature, the broadening increasing at higher temperature. The asymmetric broadening of the peaks suggests the presence of electrical processes in the material with a spread of relaxation time (Suman *et al* 2006). In a relaxation system, one can determine the most probable relaxation time (τ) from the position of the loss peak in the Z'' vs log (f) plots according to the relation

$$\tau = 1/\omega = 1/2\pi f,$$

where f is the relaxation frequency.

Figure 9 shows the variation of relaxation time {ln (τ_b)} with $10^3/T$ (K^{-1}). It appears to follow the Arrhenius relation,

$$\tau_b = \tau_0 \exp\left(\frac{-E_a}{k_B T}\right),$$

where τ_0 is the pre-exponential factor, k_B the Boltzmann constant and T the absolute temperature. The value of activation energy (E_a) as calculated from the slope of ln (τ_b) vs $10^3/T$ curve is found to be 1·53 eV. The value of activation energy (E_a) for undoped sample is reported to be 1·56 eV (Morrison *et al* 1999). Thus, the activation energy changes by small amount on tungsten substitution. A reduced activation energy implies higher mobility of the oxygen vacancies. In these materials, oxygen vacancies are considered as one of
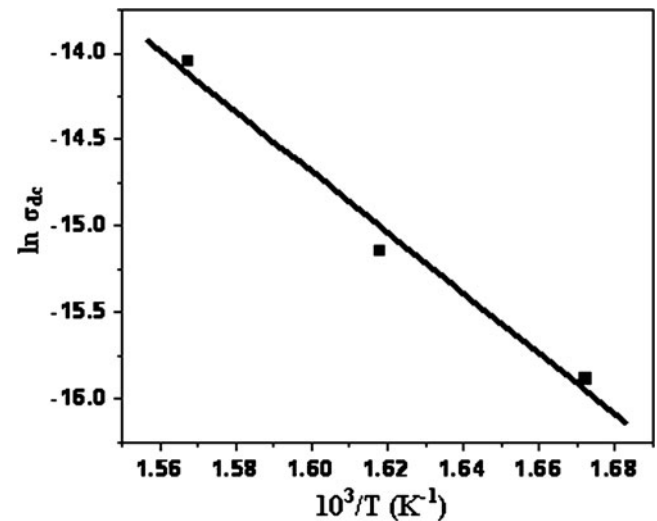

Figure 11. Variation of d.c. conductivity (σ_{dc}) with inverse of temperature ($10^3/T$).

the mobile charge carriers (Smyth 1991). The ionization of oxygen vacancies creates conduction electrons, which are easily thermally activated (Warren *et al* 1996). Thus the increase in conduction at higher temperature can be understood.

Figure 10 shows the plot of Z′ vs Z″ (Cole–Cole plots) taken over a frequency range of 20 Hz–1 MHz at different temperatures (325 °C, 345 °C, 365 °C). This range of temperature was selected as semicircles are formed in the Nyquist plots in this range. All the semicircles exhibit some depression instead of semicircles centred on the *x*-axis. Such behaviour is indicative of non-Debye type of relaxation and it also manifests that there is a distribution of relaxation time instead of a single relaxation time in the material, as discussed earlier (Plocharski and Wieczorek 1988). The value of bulk resistance (R_b) at different temperatures have been calculated from the intercepts of semicircular arc on the real axis (Z′) and is mentioned in table 1. It is observed that R_b decreases with the rise in temperature indicating a negative temperature coefficient of resistance (NTCR) behaviour (Kidner *et al* 2007). However, the presence of two semicircles at higher temperature (365 °C) exhibits the presence of both grain (bulk property) and grain boundary effects. The high frequency semicircle corresponds to a bulk contribution and low frequency corresponds to grain boundary effect (Rahmouni *et al* 2007).

Figure 11 shows the variation of σ_{dc} with $10^3/T$ (K^{-1}). The d.c. (bulk) conductivity, σ_{dc}, of the sample has been evaluated from the impedance spectrum using the relation

$$\sigma_{dc} = \frac{t}{R_b A},$$

where R_b is the bulk resistance, *t* the thickness and *A* the area of the sample. It is observed that with increasing temperature d.c. conductivity increases confirming the negative temperature coefficient of resistance (NTCR) behaviour in the compound. The observed variation of ln σ_{dc} vs $10^3/T$ is a straight line and follows the Arrhenius relationship

$$\sigma_{dc} = \sigma_0 \exp\left(\frac{-E_a}{k_B T}\right),$$

where σ_0 is the pre-exponential factor, E_a the activation energy of the mobile charge carriers, and *T* the absolute temperature. The value of activation energy (E_a) as calculated from the ln σ_{dc} with $10^3/T$ (K^{-1}) curve is found to be 1·51 eV which is nearly the same as that obtained from the relaxation time (τ_b) vs temperature curve.

5. Conclusions

On partially replacing titanium by tungsten the barium titanate remains single phase and the tetragonal structure is retained. Well developed grains are seen in SEM micrograph of the specimen. Polarization–electric field hysteresis loop confirms the ferroelectric nature of the synthesized material at room temperature. Dielectric studies reveal the diffuse nature of ferro–paraelectric phase transition. Also, an increase in dielectric constant and decrease in Curie temperature is observed on tungsten substitution. At 365 °C the resistance due to the grain boundaries is also observed in addition to granular contribution. It is also observed that the bulk resistance decreases with increase in temperature. The d.c. conductivity is observed to increase with increasing temperature further confirming the negative temperature coefficient of resistance behaviour and temperature dependent relaxation phenomenon. The temperature dependence of the relaxation time is found to obey an Arrhenius law with an activation energy of 1·53 eV.

Acknowledgement

References

Behera B, Nayak P and Choudhary R N P 2007 *J. Alloys Compd.* **436** 226

Behera B, Nayak P and Choudhary R N P 2008 *Mater. Res. Bull.* **43** 401

Cao Wanqiang, Junwen Xiong and Sun Juanpin 2007 *Chem. Phys.* **106** 338

Coondoo Indrani, Jha A K and Aggarwal S K 2006 *J. Electroceram.* **16** 393

Coondoo Indrani, Jha A K and Aggarwal S K 2007a *Ceram. Int.* **33** 41

Coondoo Indrani, Jha A K and Aggarwal S K 2007b *Ferroelectrics* **365** 31

Devi Sheela, Ganguly P, Jain S and Jha A K 2009 *Ferroelectrics* **381** 120

Dong C 1999 *J. Appl. Crystallogr.* **32** 838

Ganguly Prasun, Jha A K and Deori K L 2008 *Solid State Commun.* **146** 472

Goodman G and Buchanan R C 1986 *Ceramic capacitor material* (New York: Marcel Dekker Inc)

Haertling G H 1999 *J. Am. Ceram. Soc.* **82** 797

Hench L L and West L K 1990 *Principles of electronic ceramics* (New York: John Wiley & Sons. Inc.) p. 244

Hu H and Krupanidhi S B 1993 *J. Appl. Phys.* **74** 3373

Jaffe B, Cook W R and Jaffe H 1971 *Piezoelectric ceramics* (London: Academic Press)

Jones R E, Mainer P D, Campbell J O and Mogab C J 1992 *Appl. Phys. Lett.* **60** 1022

Kidner N J, Meier A, Homrighaus Z J, Wessels B W, Mason T O and Garboczi E J 2007 *Thin Solid Films* **515** 4588

Megaw H D 1945 *Nature (London)* **155** 484

Merz W J 1949 *Phys. Rev.* **76** 1221

Morrison Finlay D, Sinclair Derek C and West Anthony R 1999 *J. Appl. Phys.* **86** 6355

Pilgrim S M, Sutherland A E and Winzer S R 1990 *J. Am. Ceram. Soc.* **73** 3122

Plocharski J and Wieczorek W 1988 *Solid State Ionics* **28–30** 979

Rahmouni H, Nouiri M, Jemai R, Kallal N, Rzigua F, Selmi A, Khirouni K and Alaya S 2007 *J. Magn. Magn. Mater.* **316** 23

Reynolds T G 2001 *Am. Ceram. Soc. Bull.* **80** 29

Sen S, Pramanik P and Choudhary R N P 2007 *Physica* **B387** 52

Shannon R D and Prewitt C T 1969 *Acta Crystallogr.* **B25** 925

Sinclair D C and West A R 1989 *J. Appl. Phys.* **66** 3850

Sinclair D C and West A R 1994 *J. Mater. Sci.* **29** 6061

Smyth D M 1991 *Ferroelectrics* **117** 117

Stojanovic B D, Foschini C R, Pejovic V Z, Pavloic V B and Varela J A 2004 *J. Eur. Ceram. Soc.* **24** 1467

Suman C K, Prasad K and Choudhary R N P 2006 *J. Mater. Sci.* **41** 369

Uchino K and Nomura S 1982 *Ferroelectr. Lett. Sect.* **44** 55

Venkateswarlu P, Laha Apurba and Krupanidhi S B 2005 *Thin Solid Films* **474** 1

Viswanath R N and Ramasamy S 1997 *Nanostruct. Mater.* **8** 155

Warren W L, Vanheusden Dimos K D, Pike G E and Tuttle B A 1996 *J. Am. Ceram. Soc.* **79** 536

Wu Y, Limmer S J, Chou T P, Nguyen C and Cao G 2002 *J. Mater. Sci. Lett.* **21** 947

Xiong J W, Zeng B and Cao W Q 2004 *J. Electroceram.* **52** 5177

Zaffe B, Cook Jr W R and Jaffe H 1971 *Piezoelectric ceramics* (London: Academic Press)

Zhang L, Zhao S, Yu H, Zheng L, Li G and Yin Q 2004 *Jap. J. Appl. Phys.* **43** 7613

Zong Ximei, Yang Z, Hui Li and Yuan M 2004 *Mater. Res. Bull.* **39** 175